Label-Free Biosensors Based on Aptamer-Modified Graphene Field-Effect Transistors

Ohno, Y.; ***Maehashi, K.***; ***Matsumoto, K.***
(The Institute of Scientific and Industrial Research)

Journal of the American Chemical Society, **132,** 18012-18013 (2010)

A label-free immunosensor based on an aptamer-modified graphene field-effect transistor (G-FET) is demonstrated. Immunoglobulin E (IgE) aptamers with approximate height of 3 nm were successfully immobilized on a graphene surface, as confirmed by atomic force microscopy. The aptamer-modified G-FET showed selective electrical detection of IgE protein. From the dependence of the drain current variation on IgE concentration, the dissociation constant was estimated to be 47 nM, indicating good affinity and the potential for G-FETs to be used in biological sensors.

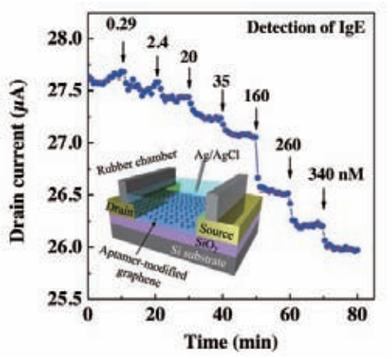

Stimulated Raman Scattering Microscope with Shot Noise Limited Sensitivity Using Subharmonically Synchronized Laser Pulses

Ozeki, Y.; ***Kitagawa, Y.***; ***Sumimura, S***; ***Nishizawa, N.***; ***Umemura, W.***; Kajiyama, S.; ***Fukui, K.***; ***Itoh, K.***
(Graduate School of Engineering)

Optics Express**, 18,** 13708-13719 (2010)

Stimulated Raman scattering (SRS) microscopy allows label-free imaging of live cells and tissues with high contrast. However, an important issue of SRS microscopy has been its sensitivity because SRS signal is deteriorated by laser noise. This paper demonstrates that the sensitivity limit can be achieved by using subharmonically synchronized two-color lasers. Experimentally, 38-MHz Yb-fiber laser pulses are successfully synchronized to 76-MHz Ti:sapphire laser pulses. By using these pulses, high-frequency lock-in detection of SRS signal is accomplished, and the effect of low-frequency laser noise is significantly suppressed. The noise level is found to be higher than the theoretical limit only by 1.6 dB. We also demonstrate high-contrast, 3D imaging of unlabeled living cells.

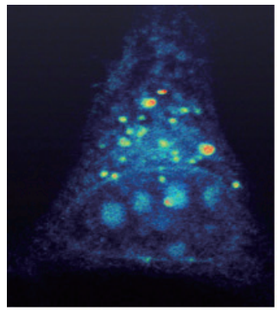

Prediction of Greenhouse Gas Reduction Potential in Japanese Residential Sector by Residential Energy End-use Model

Shimoda, Y.; Yamaguchi, Y.; Okamura, T.; Taniguchi, A.; ***Yamaguchi, Y.***
(Graduate School of Engineering)

Applied Energy, **87,** 1944-1952(2010)

A model was developed that simulates nationwide energy consumption of the residential sector by considering the diversity of household and building types. Since this model can simulate the energy consumption for each household category based on the schedule of the occupants' activities and a dynamic heat transfer model, various kinds of energy-saving policies can be evaluated with considerable accuracy. In this paper, energy consumption and CO_2 emissions in the Japanese residential sector until 2025 were predicted. For example, as a business-as-usual case, CO_2 emissions will be reduced by 7% from the 1990 level. Additional mitigation measures such as dissemination of photovoltaic panels were also evaluated.

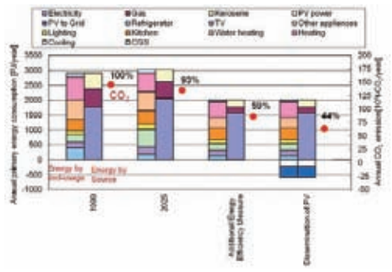

One-Pot Synthesis of Benzimidazoles by Simultaneous Photocatalytic and Catalytic Reactions on Pt@TiO_2 Nanoparticles

Shiraishi, Y.; ***Sugano, Y.***; Tanaka, S.; ***Hirai, T.***
(Research Center for Solar Energy Chemistry)

Angewandte Chemie International Edition**, 49,** 1656-1660 (2010)

Benzimidazole and its derivatives have attracted a great deal of attention because of their biological activities against several viruses such as HIV, herpes, and influenza. These compounds are however usually synthesized under strong acidic conditions and high temperature (ca. >200 °C). We developed an efficient and selective benzimidazole production process by photoirradiation (λ>300 nm) of alcohol solutions containing ***o-***arylenediamines with TiO_2 loading Pt nanoparticles (Pt@TiO_2) at room temperature. This is promoted by one-pot catalytic transformations on the catalyst via a Pt-assisted photocatalytic oxidation of alcohols and a catalytic dehydrogenation of the intermediates on the surface of Pt nanoparticles.

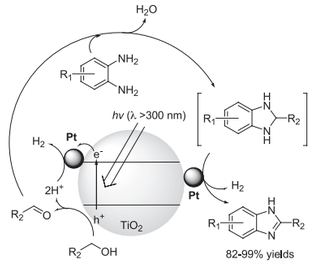

Three-Dimensional Electron Density Mapping of Shape-Controlled Nanoparticle by Focused Hard X-ray Diffraction Microscopy

Takahashi, Y.; ***Zettsu, N.***; Nishino, Y.; ***Tsutsumi, R.***; Matsubara, E.; Ishikawa, T.; ***Yamauchi, K.***
(Graduate School of Engineering)

Nano Letters**, 10,** 1922-1926 (2010)

Coherent diffraction microscopy using highly focused hard X-ray beams allows us to three-dimensionally observe thick objects with a high spatial resolution, also providing us with unique structural information, i.e., electron density distribution, not obtained by X-ray tomography with lenses, atom probe microscopy, or electron tomography. We measured high-contrast coherent X-ray diffraction patterns of a shape-controlled Au/Ag nanoparticle and successfully reconstructed a projection and a three-dimensional image of the nanoparticle with a single pixel (or a voxel) size of 4.2 nm in each dimension. The small pits on the surface and a hollow interior were clearly visible. The Au-rich regions were identified based on the electron density distribution, which provided insight into the formation of Au/Ag nanoboxes.

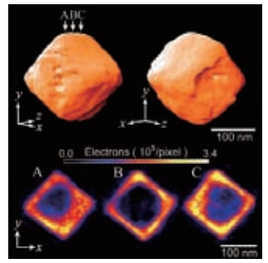

Low Young's Modulus of Ti–Nb–Ta–Zr alloys Caused by Softening in Shear Moduli c' and c_{44} near Lower Limit of Body-centered Cubic Phase Stability

Tane, M.[*1]; Akita, S.; ***Nakano, T.***[*2]; ***Hagihara, K.***[*2]; Umakoshi, Y.; Niinomi, M.; ***Mori, H.***[*3]; ***Nakajima, H.***[*1]
[*1](The Institute of Scientific and Industrial Research)
[*2](Graduate School of Engineering)
[*3](Research Center for Ultra-High Voltage Electron Microscopy)

Acta Materialia, **58,** 6970-6978 (2010)

The origin of low Young's modulus in Ti-Nb-Ta-Zr β-phase alloys with a body-centered cubic structure, developed for biomedical applications, was investigated using their single crystals. Electromagnetic acoustic resonance measurements clarified that the shear moduli c' and c_{44} of single crystals soften upon cooling from room temperature and become rather low near the lower limit of β-phase stability. An analysis by the Hill approximation indicates that low c' and c_{44} caused their softening near the lower limit of β-phase stability is the origin of low Young's modulus.

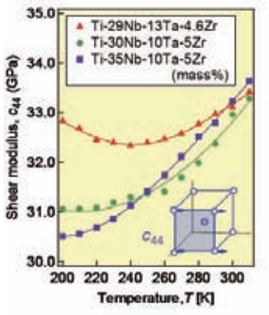

▲Reprinted from ***Acta Materialia,*** 58, M. Tane et al., Low Young's modulus of Ti–Nb–Ta–Zr alloys caused by softening in shear moduli c' and c_{44} near lower limit of body-centered cubic phase Stability, 6790-6798, Copyright(2010), with permission from Elsevier.

Verification of Consensus Algorithms Using Satisfiability Solving

Tsuchiya, T.; Schiper, A.
(Graduate School of Information Science and Technology)

Distributed Computing**, 23,** 341-358 (2011)

Consensus, the problem of getting all computing nodes in a network to agree on the same decision, is at the heart of many mission-critical computing systems. This paper presents a semi-automatic verification approach for consensus algorithms. The approach uses model checking, which is a state traversal-based verification method. The challenge here is that the state space of these algorithms is often infinite, making this method infeasible. The proposed approach addresses this difficulty by reducing the verification problem to a set of small model checking problems by making use of structural properties of this particular class of algorithms.

Execution time (h:m:s) and the maximum number of processes for which the verification was successful.

Tool	Agreement verification		Termination verification	
Proposed approach	9 nodes	2:10:14	14 nodes	4:04:35
NuSMV	4 nodes	0:02:47	3 nodes	0:00:41
SPIN	3 nodes	0:48:42	-	-
ALV	3 nodes	0:32:01	-	-

Oxidant-Free Direct Coupling of Internal Alkynes and 2-Alkylpyridine via Double C-H Activations by Alkylhafnium Complexes

Tsurugi, H.; ***Yamamoto, K.***; ***Mashima, K.***
(Graduate School of Engineering Science)

Journal of the American Chemical Society, **133,** 732-735 (2011)

The development of new methods for selective syntheses of functionalized carbocycles with a controlled configuration is important due to the presence of these skeletons in biologically relevant compounds. We recently found a coupling reaction of 2,6-lutidine and internal alkynes leading to five-membered carbocyclic compounds by non-metallocene cationic hafnium-alkyl complexes as a first example of an oxidant-free cross dehydrogenative coupling reaction. Formally, the methyl group of 2,6-lutidine becomes a C1 source of the [2+2+1] cyclization reaction through the activation of two carbon-hydrogen bonds of the methyl group, and the double C-H activation on the same carbon atom is a new strategy for generating C1 sources for various coupling reactions.